Noise from Imperfectly Expanded Supersonic Coaxial Jets

Marco Debiasi[*] and Dimitri Papamoschou[†]
University of California, Irvine, Irvine, California 92697-3975

Experiments have characterized the acoustics of axisymmetric high-speed jets at a variety of Mach numbers and velocities and at pressure-matched, overexpanded, and underexpanded conditions. The effect of an annular secondary flow on noise emission was also investigated. The fully expanded jet velocity ranged from 630 to 920 m/s and the fully expanded jet Mach number ranged from 1.27 to 1.75. The secondary flow was supplied at 400 m/s and was designed for Mach wave elimination conditions. Imperfect expansion creates screech and broadband shock noise. Screech is dominant in the near field whereas broadband shock noise affects mainly the lateral direction of the far field. The secondary flow practically eliminates the screech tones, but has little impact on broadband shock noise. With exception of localized and weak screech tones, the far-field spectra in the direction of peak noise emission (aft quadrant) are insensitive on nozzle exit pressure and depend solely on the fully expanded Mach number and velocity. Addition of the secondary flow produces substantial noise reduction in the aft quadrant, a consequence of Mach wave elimination, and modest noise reduction in the lateral direction, an effect attributed to mean shear reduction. Lowering the velocity and/or Mach number of the jet enhances the benefit of the secondary flow by shortening the region of the principal noise sources, thus improving the coverage of that region by the secondary flow. Far-field noise reductions of up to 17 dB were recorded at frequencies most relevant to aircraft noise.

I. Introduction

EFFICIENT suppression of high-speed jet noise remains an unsolved problem that has prevented wide-scale development of supersonic transports. Supersonic jet noise consists of three main components: turbulent mixing noise, screech tones, and broadband shock noise.[1] The latter two are associated with the shock cell system in imperfectly expanded jets. In high-speed jets, mixing noise is dominated by Mach wave emission, which radiates in the downstream direction and is caused by the supersonic convection of eddies relative to their surrounding medium. Mach wave radiation has been the subject of numerous analytical, computational, and experimental investigations, for example, see Refs. 1–6. There is wide agreement that Mach wave emission is a phenomenon associated with an instability wave propagating at supersonic speed. Reducing Mach wave emission is a key challenge for making high-speed transports environmentally acceptable.[7] In addition, Mach wave radiation can induce sonic fatigue of aircraft structures;[8] thus, its near-field suppression is also important.

Screech is a discrete tone emitted by imperfectly expanded jets. It has a significant upstream propagation component and, thus, can cause damage to the engine nozzle structure.[9] Screech is thought to be generated and sustained by a resonant feedback loop that comprises the following elements: 1) sound generated by passage of eddies through shock cells, 2) upstream propagation of the sound toward the nozzle lip, and 3) generation of a new eddy by coupling of the sound with the shear-layer instability.[10–12] The second component of shock-associated noise is broadband in nature and propagates in the lateral and upstream directions. Its spectral amplitude rises rapidly with frequency to a main peak and then decreases at higher frequencies. Broadband shock noise is believed to consist of acoustic waves generated by supersonically convecting, coherent, wavelike disturbances arising from the interaction of large-scale turbulent structures with the nearly periodic shock cell system of imperfectly expanded jets.[13–15]

Recently, it was demonstrated that addition of a secondary flow to a supersonic jet can reduce Mach wave emission when the convective velocity of the jet eddies with respect to the secondary flow drops to subsonic values, provided that the secondary flow eddies are also subsonic with respect to the ambient.[16,17] This method, called Mach wave elimination, achieved appreciable noise reduction in a pressure-matched jet with velocity of 920 m/s (Ref. 17). It was evident that further refinement of the method entailed better knowledge of the acoustic field of the primary jet and its dependence on nozzle exit parameters, as well as better understanding of the interaction of the secondary flow with the jet. Specifically, the effects of exit Mach number and velocity on the noise characteristics of single and coaxial jets warranted examination. In addition, it was important to assess the impact of the secondary flow on noise sources not present in previous experiments, namely, those arising from imperfect expansion of the jet. The present work attempts to address these issues with the measurement of noise from a large variety of single and coaxial jets.

II. Flow Conditions

Experiments were conducted in a coaxial jet facility detailed in Ref. 16. Mixtures of helium and air were supplied to a concentric nozzle arrangement shown in Fig. 1. Subscripts 1, 2, and ∞ refer to the jet, secondary flow, and ambient conditions, respectively. Two inner nozzles, of 12.7 mm exit diameter, were designed by the method of characteristics for Mach numbers $M_1 = 1.5$ and 1.75. Schlieren visualization and pitot pressure profiles at the nozzle exit indicated no significant presence of shocks when the nozzles were operated at pressure-matched conditions. The outer nozzle had a conical convergent shape and terminated in an exit diameter of 25.4 mm. Precisely metered mixtures of helium and air were supplied to the nozzles, which exhausted into ambient, still air. Helium–air mixtures simulate adequately the density, velocity, and speed of sound of a heated jet.[18] When the mass fractions of helium and air are regulated, thereby regulating the gas constant of the mixture, we controlled the jet velocity at a given Mach number. The facility was equipped with pressure transducers that recorded the total pressures of the jet and secondary flow streams.

The investigative approach was to create several sets of jets, each set having the same fully expanded velocity. Within each set we varied the nozzle geometry and nozzle pressure ratio to generate perfectly and imperfectly expanded jets at various Mach numbers. Table 1 summarizes the flow conditions. Each jet is identified by a code, listed in the first column, which consists of a two-letter prefix

Table 1   Jet conditions

Case	M_1	U_1, m/s	p_1/p_∞	M_{1fe}	U_{1fe}, m/s	D_{1fe}, mm	$M_{c,sym}$
OE630	1.50	700	0.71	1.27	630	12.0	0.75
PM630	1.50	630	1.00	1.50	630	12.7	0.82
OE700	1.75	770	0.68	1.50	700	11.7	0.86
PM700A	1.50	700	1.00	1.50	700	12.7	0.86
PM700B	1.75	700	1.00	1.75	700	12.7	0.94
UE700	1.50	640	1.45	1.75	700	13.6	0.94
OE920	1.75	1010	0.67	1.50	920	11.7	0.96
PM920	1.50	920	1.00	1.50	920	12.7	0.96
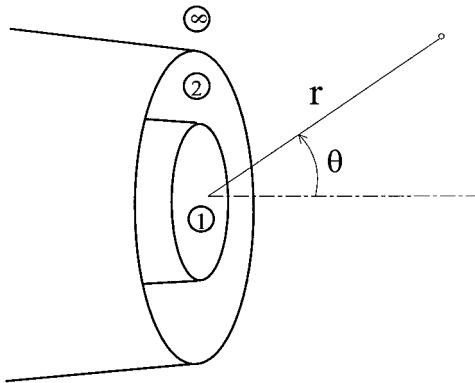
Fig. 1   Coaxial nozzle arrangement; nozzle diameters: $D_1 = 12.7$ and $D_2 = 25.4$ mm.

[overexpanded (OE), pressure matched (PM), and underexpanded (UE)] followed by the value of the fully expanded velocity in meter per second. The following three columns provide the nozzle-exit values of Mach number M_1, velocity U_1, and pressure ratio p_1/p_∞. The next three columns list the values of the fully (isentropically) expanded jet Mach number M_{1fe}, jet velocity U_{1fe}, and jet diameter D_{1fe}. The last column presents the symmetric convective Mach number $M_{c,sym} = U_{1fe}/(a_{1fe} + a_\infty)$, which is a measure of the overall compressibility of the jet; its significance will be discussed in Sec. V. The Reynolds number of the jet, based on its exit diameter D_1, ranged from a minimum of 2.75×10^5 in jet OE630 to a maximum of 5×10^5 in jet PM700B.

The secondary flow used in treating all of the jets had Mach number $M_2 = 0.84$ and velocity $U_2 = 400$ m/s and is identified by the code C400. Coaxial jets (combinations of jet and secondary flow) are identified by the jet code and secondary flow code, for example, PM920-C400. The thrust of the secondary flow is equal to the thrust of the $M_1 = 1.5$ perfectly expanded jets, and its mass flow rate is 1.7 times that of case PM700A. All of the coaxial jets satisfy the Mach wave elimination criteria of Ref. 16.

III.   Sound Measurement

Noise measurements were conducted inside an anechoic chamber using a $\frac{1}{8}$-in. condenser microphone (Brüel and Kjær 4138) with frequency response of 150 kHz. The microphone signal was sampled at 400 kHz, and the power spectrum of each record was computed using a 512-point fast Fourier transform. The microphone was mounted on an arm, which pivoted around an axis passing through the center of the jet exit. This arrangement enabled sound measurement at a variety of radial r and polar θ positions, with r ranging from 0.038 to 1.52 m and θ ranging from 20 to 100 deg, measured counterclockwise from the jet axis. For a detailed description of this setup the reader is referred to Ref. 17.

Central to our measurements is the spectrum of sound pressure level (SPL), in decibel per hertz, obtained from the relation

$$SPL(f) = 10 \log_{10} S(f)$$

where f is frequency and $S(f)$ is the power spectrum of p'/p_{ref}, with p' the pressure fluctuation and $p_{ref} = 20\,\mu$Pa the commonly used reference pressure. The power spectrum is corrected for the

transducer characteristic and the free-field response of the microphone as explained in Ref. 17. The spectra are plotted vs the Strouhal number defined as $Sr = f D_1/U_1$ for PM jets and $Sr = f D_{1fe}/U_{1fe}$ for imperfectly expanded jets.

The overall sound pressure level (OASPL) in decibel is calculated from

$$OASPL = 10 \log_{10} \int_0^{150\,kHz} S(f)\,df$$

where the upper limit of the integration is dictated by the frequency response of the microphone. Even though OASPL describes the total sound intensity at a given point, it is very inadequate as a measure of perceived noise. Sounds with the same OASPL can have variations of up to 17 dB in perceived noise depending on their spectral content.[19] For this reason, we compute another significant quantity, which is the value of the SPL spectrum at $f = 100$ kHz, denoted $SPL_{100-kHz}$. When it is considered that the diameter of our jet is 50–100 times smaller than the typical exhaust diameter of a supersonic engine, a frequency of 100 kHz measured in our experiment corresponds to a frequency range of 1000–2000 Hz in a full-scale engine, that is, the frequency range of maximum annoyance to humans, which is weighed heavily in perceived noise metrics.[19] The 100-kHz component (in decibel) is defined here as the average spectral value of the bandwidth 100 ± 13 kHz,

$$SPL_{100-kHz} = 10 \log_{10}\left[\frac{1}{\Delta f} \int_{f_0 - \Delta f/2}^{f_0 + \Delta f/2} S(f)\,df\right]$$

with $f_0 = 100$ kHz and $\Delta f = 26$ kHz. In addition to the $SPL_{100-kHz}$ metric, we also computed the A-weighted, $\frac{1}{3}$-octave spectrum, which is used widely in industry for assessment of perceived noise.[19] The conversion of the narrowband spectra to the so-called dBA scale is outlined in Ref. 17. For subscale experiments such as ours, it entails an assumption about the size of the actual engine exhaust. Because this work focuses more on the physics of sound emission than on design of engine configurations, we will show dBA spectra only for selected cases.

Atmospheric absorption has modest impact on the spectral shapes and affects only the high frequencies. At $f = 100$ kHz, absorption has negligible effect on the near-field SPL and an impact of at most 2.5 dB on the far-field SPL (assuming a relative humidity of 40%, which is largest value recorded inside our anechoic chamber). It is not a significant correction as far as the scope of this work is concerned, and so it has not been applied to the spectra presented here.

All of the noise data are corrected to equal thrust by using the geometric scaling outlined in Ref. 17. For given exhaust conditions, the sound intensity at a fixed point scales directly with D^2 (Ref. 20). The nozzle thrust also scales with D^2. The equal-thrust correction entails scaling up or down the diameter of a given jet so that its thrust matches that of a reference jet, in this case PM920. The corrected sound intensity is, thus, the actual sound intensity divided by the thrust ratio between this jet and the reference jet.

IV.   Results

This section will focus on a description of the noise spectra in two key directions: peak noise emission and lateral. The direction of peak emission is defined as the direction of maximum OASPL; it always occurred in the aft quadrant at an angle $\theta = \theta_{peak}$, dependent primarily on the jet velocity. The lateral direction is defined here as $\theta = 100$ deg, which is the largest polar angle achievable with the present microphone setup; it is the direction in which screech and broadband noise are most dominant. For brevity, we will present only selected spectra that are representative of the trends observed in all of the cases. Summary values (far-field OASPL and $SPL_{100-kHz}$ in two directions) for all of the jets are given in Table 2. Table 2 includes the prediction of the actual convective Mach number M_c of the jet eddies with respect to their surrounding medium: ambient for single jets and secondary flow for coaxial jets. The value of M_c for secondary flow C400, with respect to the ambient, was 0.70. The convective Mach number was calculated using the empirical

Table 2 Far-field noise data

Case	M_{1fe}	U_{1fe}	M_c	$\theta = \theta_{peak}$		$\theta = 100$ deg	
				OASPL, dB	SPL$_{100\text{-kHz}}$, dB	OASPL, dB	SPL$_{100\text{-kHz}}$, dB
OE630	1.27	630	1.31	125.81	58.97	111.26	55.73
OE630-C400	1.27	630	0.24	126.64	41.08	111.47	48.02
PM630	1.50	630	1.06	129.63	63.84	114.14	57.44
PM630-C400	1.50	630	0.26	131.13	50.46	119.91	57.09
OE700	1.50	700	1.54	132.57	67.24	118.17	59.79
PM700A	1.50	700	1.54	132.67	68.04	115.21	58.52
OE700-C400	1.50	700	0.32	128.41	54.62	117.24	57.65
PM700A-C400	1.50	700	0.32	129.71	55.13	116.48	56.91
UE700	1.75	700	1.66	134.60	71.83	122.87	64.72
PM700B	1.75	700	1.66	133.71	71.40	116.99	60.56
UE700-C400	1.75	700	0.35	132.15	68.02	120.37	61.29
PM700B-C400	1.75	700	0.35	131.11	67.01	116.09	58.19
OE920	1.50	920	1.82	133.98	69.92	119.33	62.47
PM920	1.50	920	1.82	134.96	69.93	118.50	59.65
OE920-C400	1.50	920	0.63	130.64	63.79	116.85	58.55
PM920-C400	1.50	920	0.63	130.09	62.91	117.54	59.23
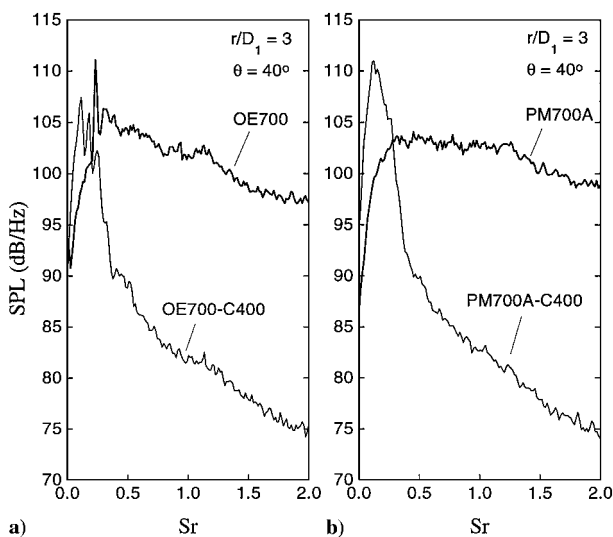
Fig. 2 Near-field spectra in the direction of peak emission for $M_{1fe} = 1.5$ and $U_{1fe} = 700$ m/s: a) OE700 and OE700-C400 and b) PM700A and PM700A-C400.

Fig. 3 Near-field spectra in the direction of peak emission for $M_{1fe} = 1.75$ and $U_{1fe} = 700$ m/s: a) UE700 and UE700-C400 and b) PM700B and PM700B-C400.

relations offered in Ref. 21, which are based on direct measurements of M_c in compressible jets and shear layers.

Direction of Peak Emission
Near-Field Spectra
We compare jets with same fully expanded velocity and Mach number but different exit pressure ratios. The effect of secondary flow C400 on each of those jets is described. Figure 2 presents the near-field spectra of OE and PM jets at same fully expanded Mach number $M_{1fe} = 1.5$ and velocity $U_{1fe} = 700$ m/s (cases OE700 and PM700A). When the spectra of OE700 and PM700A are compared, we note that overexpansion produces a screech tone at $Sr = 0.25$. The secondary flow eliminates the screech tone and lowers the spectrum substantially, by as much as 20 dB, in the mid-to-high frequencies. The spectrum of OE700-C400 displays a broad peak centered at $Sr = 0.15$, which has the appearance of broadband shock noise but whose source is not clear. A similar peak will show up in several other cases and will be discussed later. In the PM case PM700A (Fig. 2b), addition of the secondary flow reduces the spectral components above $Sr = 0.5$ by roughly the same amount as in OE700, but the low-frequency peak was amplified. Figure 3 shows UE and PM jets at equal fully expanded Mach number $M_{1fe} = 1.75$ and velocity $U_{1fe} = 700$ m/s (cases UE700 and PM700B). With exception of the screech tone of UE700, the spectra of UE700 and PM700B are otherwise quite similar. As in the cases examined earlier, the secondary flow suppresses the screech tone but introduces a broader peak of roughly the same amplitude as the screech tone. A comparable peak
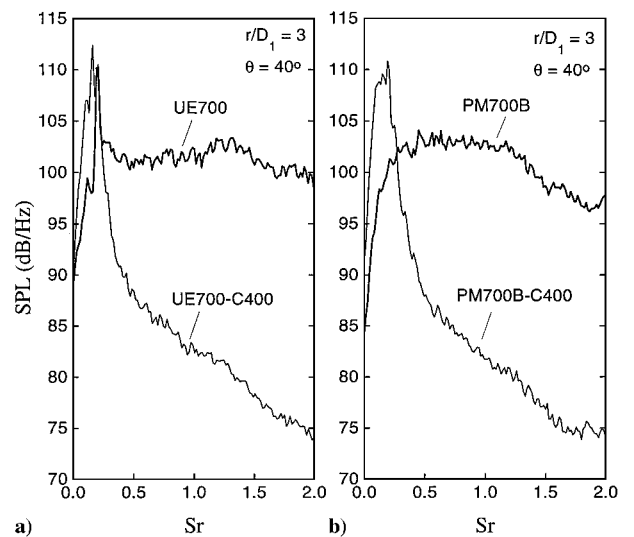
is seen in the PM jet (Fig. 3b). The mid-to-high-frequency noise components were reduced by about 20 dB in both the UE and PM jets.

The spectra of higher speed jets, cases OE920 and PM920, are shown in Fig. 4. Notable is the absence of screech tones in the OE jet OE920; this agrees with the finding by Krothapalli and Strykowski[22] and Krothapalli et al.[23] that the loss of axisymmetric coherence with increasing jet temperature (decreasing density) weakens the feedback loop that sustains screech, thereby reducing or eliminating the screech tones. The spectra of OE920 and PM920 are, thus, virtually identical. However, the spectrum of the coaxial jet OE920-C400 presents an unusual knee at $Sr = 1.0$ with no further reduction of the higher frequency components. This result, obtained consistently when repeating our measurement, needs further investigation to be explained.

Far-Field Spectra
The far-field spectra of cases OE700 and PM700A are practically identical, as shown in Figs. 5a and 5b. The same holds for the spectra of the coaxial jets OE700-C400 and PM700A-C400 also shown in Figs. 5a and 5b. At $Sr = 0.25$, the OE jet OE700 presents a small remnant of the screech tone noted in the near field. The tone vanishes with application of the secondary flow. The noise reduction at the higher frequencies reaches 13 dB for $Sr > 1$, an effect of Mach wave elimination. The far-field spectra of higher Mach number jets UE700 and PM700B (shown in Fig. 6) are also very similar. This suggests that the far-field noise is insensitive on
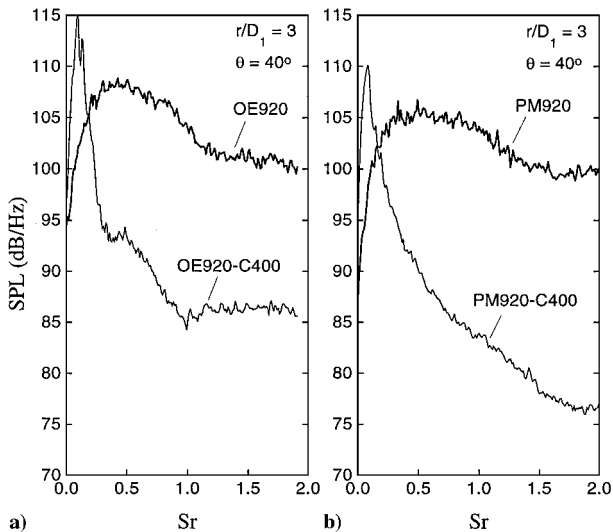
Fig. 4   Near-field spectra in the direction of peak emission for $M_{1fe} = 1.5$ and $U_{1fe} = 920$ m/s: a) OE920 and OE920-C400 and b) PM920 and PM920-C400.
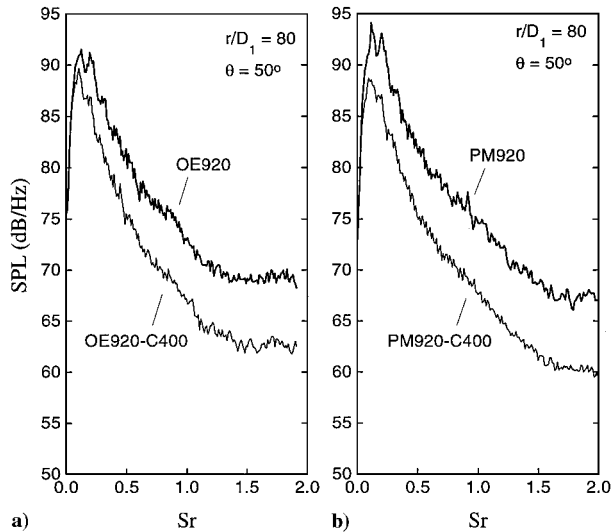
Fig. 7   Far-field spectra in the direction of peak emission for $M_{1fe} = 1.5$ and $U_{1fe} = 920$ m/s: a) OE920 and OE920-C400 and b) PM920 and PM920-C400.
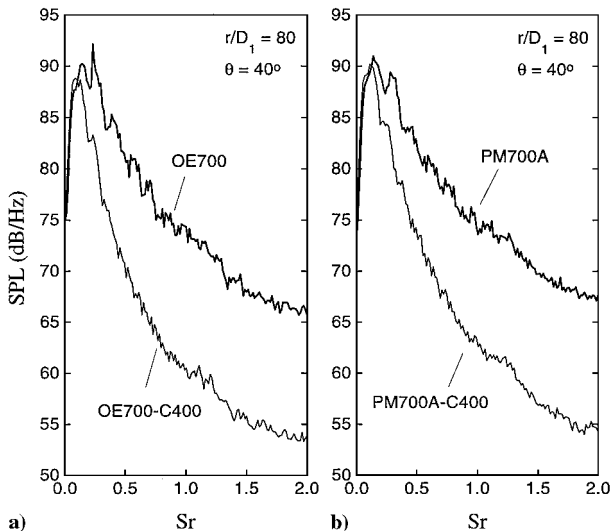
Fig. 5   Far-field spectra in the direction of peak emission for $M_{1fe} = 1.5$ and $U_{1fe} = 700$ m/s: a) OE700 and OE700-C400 and b) PM700A and PM700A-C400.
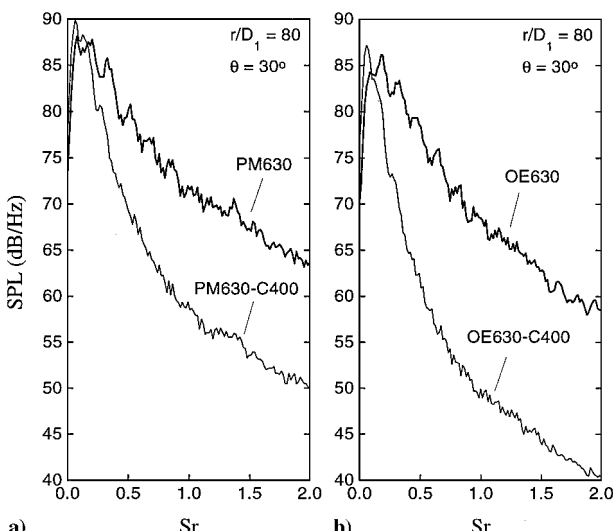
Fig. 8   Far-field spectra in the direction of peak emission for $U_{1fe} = 630$ m/s: a) OE630 and OE630-C400 ($M_{1fe} = 1.27$) and b) PM630 and PM630-C400 ($M_{1fe} = 1.5$).
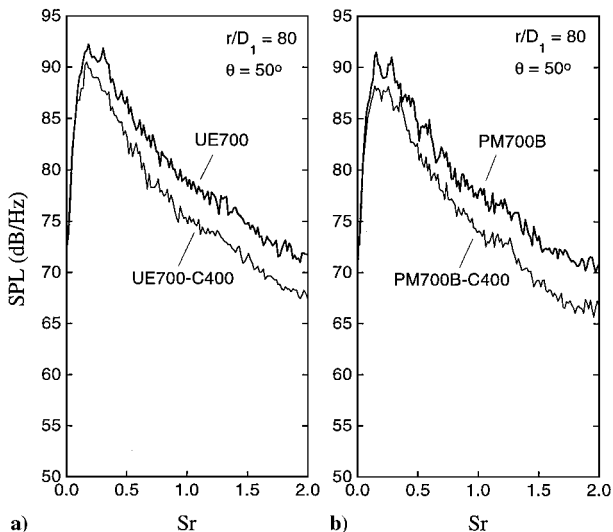
the flow condition at the nozzle exit, in agreement with the recent findings of Tam[24] that the characteristics of the jet at the nozzle exit have very small influence on the far-field noise components generated by the large turbulent structures of the flow. Comparing the coaxial jets of Figs. 5 and 6, it is evident that the ability of the secondary flow to reduce Mach wave emission is weakened with increasing jet Mach number. This is believed to be a consequence of the elongation of the Mach wave emitting region of the jet with increasing M_{1fe}, an effect that will be elaborated upon in Sec. V.

The far-field spectra of higher velocity cases OE920 and PM920 are shown in Fig. 7. As in the preceding cases, the similarity of the corresponding spectra support the concept that the far-field noise is independent of the degree of expansion at the nozzle exit. Application of the secondary flow to these jets reduced the high-frequency spectral components by 7 dB. A final comparison is made between the lower speed jets OE630 and PM630, shown in Fig. 8. In contrast to the earlier comparisons, the fully expanded Mach number was not the same in these two cases: It equaled 1.50 in PM630 and 1.27 in OE630. The purpose of this comparison is to illustrate the strong effect of jet Mach number (at fixed jet velocity) on the noise emission and its suppression using a secondary flow. The spectrum of OE630 is about 5 dB lower than that of

Fig. 6   Far-field spectra in the direction of peak emission for $M_{1fe} = 1.75$ and $U_{1fe} = 700$ m/s: a) UE700 and UE700-C400 and b) PM700B and PM700B-C400.
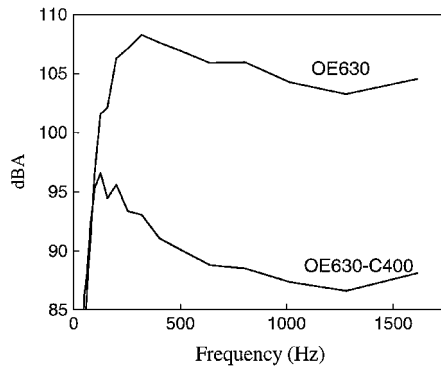
Fig. 9   A-weighted spectra of cases OE630 and OE630-C400 scaled for a jet diameter of 1 m.

PM630. At $Sr = 2.0$, the noise reduction using the secondary flow is 12 dB for PM630-C400 and 17 dB for OE630-C400. The combined benefit of lowering the jet Mach number from 1.50 to 1.27 is around 10 dB. See Sec. V for a more detailed discussion of this effect.

An overall assessment of the effects of the fully expanded values of velocity and Mach number on the far-field peak noise emission can be obtained by comparing Figs. 5–8, as well as the noise values listed in Table 2. The spectral peaks decline with decreasing U_{1fe}, although this drop is marginal. The secondary flow was most effective in reducing the noise of jets with fully expanded velocity 700 and 630 m/s, producing a drop of around 13 dB at the mid- and high frequencies. Higher speed jets had a long Mach wave emitting region and so this particular secondary flow had difficulty eliminating Mach waves far from the exit. Even more important is the effect of the fully expanded Mach number, a point already raised in discussing Fig. 6. It will be shown in Sec. V that decreasing the jet Mach number at fixed velocity reduces the length of the Mach wave emitting region of the jet. This reduces the noise emitted by the jet and enhances the ability of the secondary flow to eliminate Mach waves.

For a preliminary assessment of the perceived noise reduction associated with the spectra of Fig. 8b, we processed the spectra of cases OE630 and OE630-C400 into the A-weighted, $\frac{1}{3}$-octave metric assuming an engine exhaust diameter of 1 m (scale-up factor of 80). The A-weighted spectra, shown in Fig. 9, are fairly flat, in contrast with the narrowband SPL spectra, which drop rapidly with increasing frequency. Even though application of the secondary flow reduces little the peak of the narrowband spectrum, it reduces substantially, by around 12 dBA, the peak of the A-weighted spectrum. We present these A-weighted spectra not as a quantitative prediction of aircraft noise, but rather to illustrate the dramatic change in interpretation of noise data when the element of human perception is included.

Lateral Direction
Near-Field Spectra

We now focus on the lateral and slightly forward direction, $\theta = 100$ deg, where screech and broadband shock noise are more significant. We examine OE and PM jets with $M_{1fe} = 1.5$ and $U_{1fe} = 700$ m/s. Figure 10 presents the near field of these jets, without and with secondary flow. The OE single jet OE700 exhibits a very strong screech tone at $Sr = 0.25$ followed by a lower broadband peak. Application of the secondary flow effectively removes this tone, but introduces a broadband peak whose amplitude is comparable with that of the broadband noise of the single jet. This spectral feature of the coaxial jet was noted earlier in the near-field spectra in the direction of peak noise emission. The PM jet PM700A shows minor peaks at $Sr = 0.25$–0.4, possibly resulting from a slight nozzle pressure mismatch. The broadband tone associated with application of the secondary flow is of roughly the same amplitude as in OE700 and exceeds the spectral peak of PM700A by about 5 dB. At $Sr > 0.5$, the spectra of OE700 and PM700A are similar. For both jets, application of the secondary flow produces a uniform reduction of these spectral components by 6 dB.
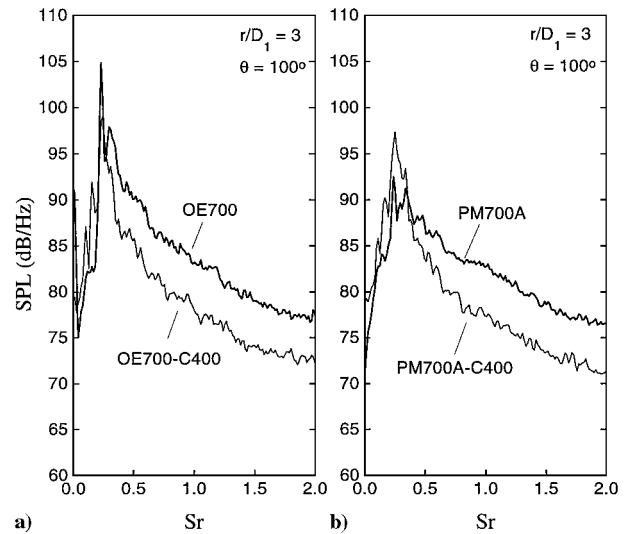
Fig. 10   Near-field spectra in the lateral direction for $M_{1fe} = 1.5$ and $U_{1fe} = 700$ m/s: a) OE700 and OE700-C400 and b) PM700A and PM700A-C400.
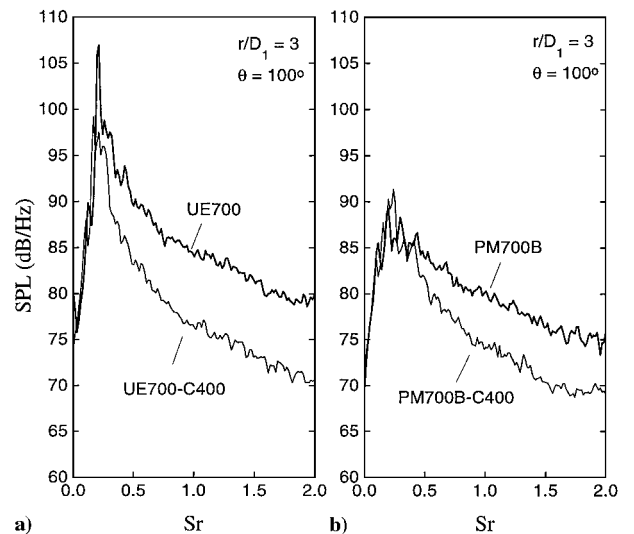
Fig. 11   Near-field spectra in the lateral direction for $M_{1fe} = 1.75$ and $U_{1fe} = 700$ m/s: a) UE700 and UE700-C400 and b) PM700B and PM700B-C400.

The spectra of UE and PM jets at $M_{1fe} = 1.75$ and $U_{1fe} = 700$ m/s are presented in Fig. 11. The trends are similar to those of Fig. 10, that is, the secondary flow removes the screech tone but introduces a broadband peak. In the PM case PM700B, however, the secondary flow does not produce any appreciable spectral peak. The higher frequency components of these jets are nearly alike with a uniform noise benefit of about 7 dB with application of the secondary flow.

Far-Field Spectra

Figure 12 shows the far-field spectra of OE700 and PM700A. The OE jet (Fig. 12a) presents a clear broadband peak. The reduction of this noise component with secondary flow is minimal, and the most noticeable change is a decrease of the broadband peak frequency, a result consistent with previous analysis by Krothapalli et al.[23] and Tam.[25] Addition of the secondary flow to the PM jet produces a broadband peak at $Sr = 0.5$, a problem already observed for the same jet in the near field. Note, however, that this noise peaks at $Sr = 0.25$ in the near field. If it comes from the same source, this suggests that the source is a convecting one. Addition of the secondary flow had minimal benefit on the higher frequency components. Similar results are seen in Fig. 13 for jets UE700 and PM700B, that is, minimal impact of the secondary flow on the broadband
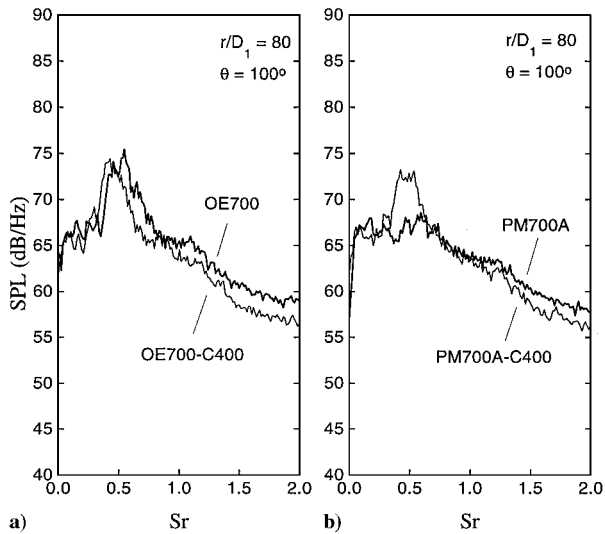
Fig. 12 Far-field spectra in the lateral direction for $M_{1fe} = 1.5$ and $U_{1fe} = 700$ m/s: a) OE700 and OE700-C400 and b) PM700A and PM700A-C400.

Fig. 13 Far-field spectra in the lateral direction for $M_{1fe} = 1.75$ and $U_{1fe} = 700$ m/s: a) UE700 and UE700-C400 and b) PM700B and PM700B-C400.
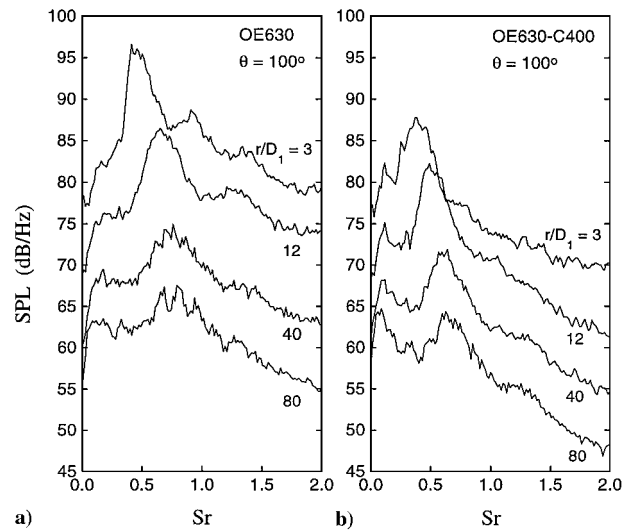
Fig. 14 Evolution of lateral spectra with radial distance for $M_{1fe} = 1.27$ and $U_{1fe} = 630$ m/s: a) OE630 and b) OE630-C400.
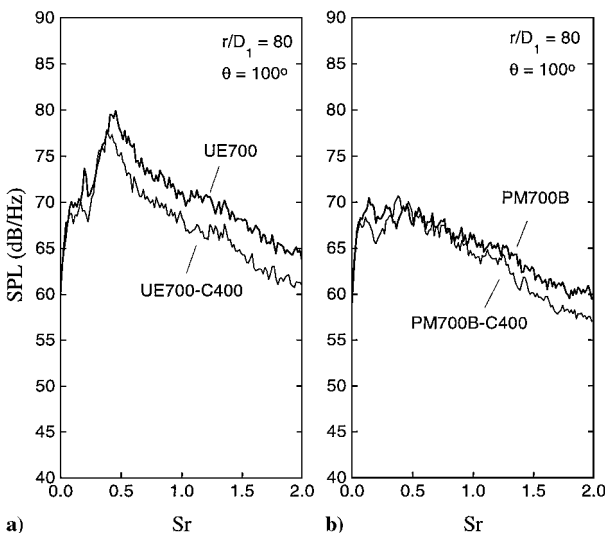
Fig. 15 Maximum value of dBA spectrum vs polar angle for cases OE630 and OE630-C400.

noise and small reduction of the mid- and high-frequency spectral components. Note the absence of tones in PM700B-C400, consistent with the near-field result of Fig. 11b.

Figure 14 presents the evolution of lateral spectra with radial distance for cases OE630 and OE630-C400. In Fig. 14a, we observe a strong broadband peak in the near field, which widens and shifts to higher frequencies with increasing distance from the nozzle. The secondary flow lowers the broadband peak in the near field, but has little effect on the broadband peak at larger distances. Comparison of Figs. 14a and 14b indicates that, as already observed, application of the secondary flow decreases the broadband peak frequency, especially in the far field. In addition, the broadband peak becomes narrower, in accordance with the trend found by Krothapalli et al.[23] and by Tam.[25] Application of the secondary flow to this lower Mach number jet produces a substantial reduction of the mid-to-high-frequency components. The far-field benefit in this case is about 10 dB, much better than that observed in Figs. 12 and 13 for higher Mach number jets. This is believed to be a consequence of the enhanced ability of the secondary flow to cover jets with a shorter potential core.

We conclude our description of far-field noise by showing the overall effect of the secondary flow on perceived noise. Figure 15 shows the variation of perceived noise, quantified as the maximum value of the far-field dBA spectrum, with polar angle for cases OE630 and OE630-C400. A scale-up factor of 80 was used in computing the dBA spectra. The purpose of Fig. 15 is to show that secondary flow is beneficial at all of the polar angles covered in this study and that, therefore, there are no undesirable side effects from its application. Similar behavior was observed for the other cases investigated here.

V. Discussion

The study has identified three principal phenomena that warrant further discussion: 1) the effect of jet Mach number on the noise of the single jet and on noise suppression using a secondary flow, 2) the removal of screech tones with application of the secondary flow, and 3) the occasional emission of a broadband tone with application of the secondary flow.

Correlations of jet noise with engine operating parameters (for example, see Fig. 7.7 of Ref. 26) emphasize the effect of jet exhaust velocity but tend to ignore the effect of jet Mach number. The results of this paper show that the jet Mach number can have an influence similar to or greater than that of jet velocity on noise emission of supersonic jets. This effect is attributed mainly to the growth rate reduction with increasing M_1 at a fixed U_1 (for simplicity, the analysis that follows considers PM jets but can be easily extended to imperfectly expanded jets by replacing the nozzle-exit flow parameters with the corresponding fully expanded parameters). The growth rate reduction is due to the density effect and to the compressibility effect, both strong functions of M_1. Specifically, the growth rate of a one-stream shear layer (simulating the edge of a single jet) can be expressed as[27]

$$\delta' = C\left(1 + \sqrt{\rho_\infty/\rho_1}\right) f(M_{c,sym}) \qquad (1)$$

where C is a constant that depends on the definition of thickness and $f(M_{c,sym})$ describes the stabilizing effect of the symmetric convective Mach number $M_{c,sym}$, an overall measure of shear-layer compressibility. For a single jet, $M_{c,sym}$ is

$$M_{c,sym} = U_1/(a_1 + a_\infty) = M_1/[1 + M_1(a_\infty/U_1)] \qquad (2)$$

where the last equality describes explicitly the dependence of $M_{c,sym}$ on M_1 at fixed U_1. The stabilizing effect of $M_{c,sym}$ can be approximated[28] as

$$f(M_{c,sym}) \approx 0.25 + 0.75e^{-3M_{c,sym}^2} \qquad (3)$$

When the definition of the speed of sound $a^2 = \gamma p/\rho$ is used, and the small variation of γ between jet and freestream is neglected in our experiments, the density ratio factor in Eq. (1) takes the form $(U_1/a_\infty)(1/M_{c,sym})$. The growth rate becomes

$$\delta' = C(U_1/a_\infty)1/M_{c,sym}\left(0.25 + 0.75e^{-3M_{c,sym}^2}\right) \qquad (4)$$

which, combined with Eq. (2), describes the stabilizing effect of M_1 on the near-field jet growth rate. It is reasonable to assume that the length of the Mach-wave-emitting region of the jet (as well as the length of all of the other significant noise sources) scales with the inverse of the growth rate. As an example, Eqs. (2) and (4) show that reducing the jet Mach number from 1.50 to 1.27, (corresponding to cases PM630 and OE630, respectively) increases the growth rate by 22%. This implies that the length of the noise-emitting region of the jet is reduced by the order of 20%, which likely accounts for OE630 being about 5 dB quieter than PM630. More important, in the case of coaxial jets, the secondary flow covers a larger portion of the noise-source region of the primary flow, giving the improved benefit evident in Fig. 8b for the direction of peak emission and in Fig. 14b for the lateral direction. The benefit in the direction of peak emission is attributed to the more complete elimination of Mach waves, especially those born near the end of the potential core. The benefit in the lateral direction, which was most noticeable in case OE630, could be due to the reduction in mean shear, which weakens the strength of the large eddies. According to Tam,[24] fine-scale noise, which is prominent in the lateral direction, is associated with small-scale turbulence, which in turn is produced by the larger structures near the end of the potential core.

The model presented here pertains to single jets. It tries to explain why a single jet at fixed velocity becomes noisier as the Mach number increases. It is also describes the degree of difficulty in covering the Mach wave emitting region by a secondary flow. A comprehensive model for the mean flow development of coaxial jets should include the effect of the secondary flow, which can reduce substantially the growth rate. This effect, however, is very complex and warrants a parametric investigation, which is beyond the scope of this study. Such investigation, is underway in our laboratory and preliminary results are already available.[29]

The removal of the screech tones with application of the Mach 0.84 secondary flow is probably the result of the cutoff in upstream communication between the shock cells and the lip of the jet nozzle. This destroys the feedback loop thought to be responsible for generation of screech. Because the secondary flow is subsonic, the shocks in the jet plume are totally reflected from the interface between jet and secondary flow, that is, stationary shocks cannot exist inside the secondary flow stream. This means that the secondary flow cannot produce screech noise; therefore, receptivity at the secondary flow nozzle lip is inconsequential.

The broadband peaks caused by application of the secondary flow, which were prominent in certain cases but absent in others, are very perplexing. A possible explanation is the slight convergence of the secondary flow stream at the nozzle exit plane (the secondary flow duct had a mean taper of 7.7 deg at the exit plane). This could compress locally the supersonic jet resulting in formation of shocks/expansions in an otherwise PM jet, or in modification of the shock cell structure in imperfectly expanded jets. Depending on the jet Mach number and degree of over/underexpansion, this effect may be more or less pronounced. For instance, it seems to be less noticeable in OE jets, whose inward-tilting exit flow is more aligned

with the convergent outer flow. The frequency increase of the broadband peaks with increasing distance in the lateral direction, noted in the discussion of Fig. 12b, suggests a Doppler effect, that is, a moving source embedded either in the jet or in the secondary flow. If nozzle geometry is the culprit, then this problem can be fixed easily by setting a parallel secondary flow at the nozzle exit. We hope to test this hypothesis in the near future.

VI. Conclusions

The noise characteristics of perfectly and imperfectly expanded, low-density supersonic jets were studied with microphone surveys of the near and far fields. Application of a high-subsonic secondary flow at conditions designed to prevent emission of Mach waves from the jet was also investigated. This is a summary of the main findings:

1) The far-field, peak noise emission is virtually independent of nozzle pressure ratio and depends solely on the fully expanded values of jet Mach number and jet velocity. This holds for both single and coaxial jets.

2) Decreasing the fully expanded jet Mach number at fixed jet velocity reduces the length of the noise-emitting region of the jet, producing a quieter jet and enhancing the ability of the secondary flow to further attenuate the jet noise.

3) In the direction of peak emission, application of the secondary flow reduces significantly the near- and far-field spectral components in the mid-to-high-frequency region. Far-field noise reductions of up to 17 dB were measured at $Sr > 0.5$.

4) In the lateral direction, imperfectly expanded jets show distinctive low-frequency screech and broadband tones. Addition of the secondary flow removes the screech tones—an effect attributed to the destruction of the feedback loop that maintains screech—but produces little benefit on the broadband noise. The secondary flow attenuates moderately the mid-to-high-frequency components in the lateral direction; reduction of mean shear is believed to be the cause of this attenuation.

5) Addition of the secondary flow to certain jets caused a broad, low-frequency spectral peak in the lateral direction. The origin of this peak is not completely understood but may be tied to the specific duct geometry of the secondary flow stream.

References

[1]Tam, C. K. W., and Chen, P., "Turbulent Mixing Noise from Supersonic Jets," *AIAA Journal*, Vol. 32, No. 9, 1994, pp. 1774–1780.

[2]Tam, C. K. W., and Burton, D. E., "Sound Generated by Instability Waves of Supersonic Flows. Part 2. Axisymmetric Jets," *Journal of Fluid Mechanics*, Vol. 138, Jan. 1984, pp. 249–271.

[3]Dahl, M. D., and Morris, P. J., "Noise from Supersonic Coaxial Jets, Part 2: Normal Velocity Profile," *Journal of Sound and Vibration*, Vol. 200, No. 5, 1997, pp. 665–699.

[4]Mitchell, B. E., Lele, S. K., and Moin, P., "Direct Computation of Mach Wave Radiation in an Axisymmetric Supersonic Jet," *AIAA Journal*, Vol. 35, No. 10, 1994, pp. 1574–1580.

[5]McLaughlin, D. K., Morrison, G. D., and Troutt, T. R., "Experiments on the Instability Waves in a Supersonic Jet and Their Acoustic Radiation," *Journal of Fluid Mechanics*, Vol. 69, No. 11, 1975, pp. 73–95.

[6]Seiner, J. M., Bhat, T. R. S., and Ponton, M. K., "Mach Wave Emission from a High-Temperature Supersonic Jet," *AIAA Journal*, Vol. 32, No. 12, 1994, pp. 2345–2350.

[7]Seiner, J. M., and Krejsa, E., "Supersonic Jet Noise and the High Speed Civil Transport," AIAA Paper 89-2358, 1989.

[8]Fenno, C. C., Bayliss, A., and Maestrello, L., "Interaction of Sound from Supersonic Jets with Nearby Structures," *AIAA Journal*, Vol. 36, No. 12, 1998, pp. 2153–2162.

[9]Hay, J. A., and Rose, E. G., "In-Flight Shock-Cell Noise," *Journal of Sound and Vibration*, Vol. 11, 1970, pp. 411–420.

[10]Powell, A., "On the Mechanism of Choked Jet Noise," *Proceedings of the Physical Society, London*, Vol. 66, 1953, pp. 1039–1056.

[11]Tam, C. K. W., "Supersonic Jet Noise," *Annual Review of Fluid Mechanics*, Vol. 27, 1995, pp. 17–43.

[12]Raman, G., "Advances in Understanding Supersonic Jet Screech," AIAA Paper 98-0279, 1998.

[13]Harper-Bourne, M., and Fisher, M. J., "The Noise from Shock Waves in Supersonic Jets," *Proceedings of the AGARD Conference on Noise Mechanisms*, CP-131, AGARD, 1973, pp. 11/1–13.

[14]Tam, C. K. W., and Tanna, H. K., "Shock Associated Noise of Supersonic Jets from Convergent–Divergent Nozzles," *Journal of Sound and Vibration*, Vol. 81, No. 3, 1982, pp. 337–358.

[15]Tam, C. K. W., "Stochastic Model Theory of Broadband Shock Associated Noise from Supersonic Jets," *Journal of Sound and Vibration*, Vol. 116, No. 2, 1987, pp. 265–302.

[16]Papamoschou, D., "Mach Wave Elimination from Supersonic Jets," *AIAA Journal*, Vol. 35, No. 10, 1997, pp. 1604–1611.

[17]Papamoschou, D., and Debiasi, M., "Noise Measurements in Supersonic Jets Treated with the Mach Wave Elimination Method," *AIAA Journal*, Vol. 37, No. 2, 1999, pp. 154–160.

[18]Kinzie, K. W., and McLaughlin, D. K., "Measurements of Supersonic Helium/Air Mixture Jets," *AIAA Journal,* Vol. 37, No. 11, 1999, pp. 1363–1369.

[19]Smith, M. J. T., *Aircraft Noise*, Cambridge Univ. Press, Cambridge, England, U.K., 1989, pp. 9, 123, 287.

[20]Goldstein, M. E., *Aeroacoustics*, 1st ed., McGraw–Hill, New York, 1976, pp. 38, 93.

[21]Murakami, E., and Papamoschou, D., "Eddy Convection in Coaxial Supersonic Jets," *AIAA Journal*, Vol. 38, No. 4, 2000, pp. 628–635.

[22]Krothapalli, A., and Strykowski, P. J., "Revisiting Screech Tones: Effects of Temperature," AIAA Paper 96-0644, 1996.

[23]Krothapalli, A., Soderman, P. T., Allen, C. S., Hayes, J. A., and Jaeger, S. M., "Flight Effects on the Far-Field Noise of a Heated Supersonic Jet," *AIAA Journal*, Vol. 35, No. 6, 1997, pp. 952–957.

[24]Tam, C. K. W., "Influence of Nozzle Geometry on the Noise of High-Speed Jets," *AIAA Journal*, Vol. 36, No. 8, 1997, pp. 1396–1400.

[25]Tam, C. K. W., "Broadband Shock-Associated Noise From Supersonic Jets in Flight," *Journal of Sound and Vibration*, Vol. 151, No. 1, 1991, pp. 131–147.

[26]Ffowcs-Williams, J. E., and Dowling, A. P., *Sound and Sources of Sound*, Wiley, New York, 1983, p. 162.

[27]Lele, S. K., "Compressibility Effects on Turbulence," *Annual Review of Fluid Mechanics*, Vol. 26, 1994, pp. 211–254.

[28]Papamoschou, D., "Entropy Production and Pressure Variation in Confined Turbulent Mixing," *AIAA Journal*, Vol. 31, No. 9, 1993, pp. 1643–1650.

[29]Murakami, E., and Papamoschou, D., "Mixing Layer Characteristics of Coaxial Supersonic Jets," AIAA Paper 2000-2060, 2000.

P. J. Morris
Associate Editor